Post-Emergency, Multi-Hazard Health Risk Assessment in Chemical Disasters (PEC)

Report on the Evaluation of Possible Damages Suffered by Chemical and Process Vessels due to Floods

Khakzad, N.; van Gelder, Pieter

Publication date
2017

Document Version
Final published version

Post-Emergency, Multi-Hazard Health Risk Assessment in Chemical Disasters
PEC

Deliverable D.B.2

Report on the Evaluation of Possible Damages Suffered by Chemical and Process Vessels due to Floods

ECHO/SUB/2015-713844-PREV11 - PEC: Post-Emergency, multi-hazard health risk assessment in Chemical disasters
Project co-funded by ECHO - Humanitarian Aid and Civil Protection

SUMMARY

In the context of natural-technological (natech) accidents, flood-induced damage of chemical and process facilities have received relatively less attention partly due to the scarcity of experimental or high resolution field observations from one hand and partly due to the rarity of such events on the other hand. In the present study, we have investigated the possible damage of a variety of chemical and process vessels such as atmospheric storage tanks as well as pressurized vertical and horizontal vessels. We have introduced a methodology based on load-resistance relationships to assess the vulnerability of vesselsi n form of fragility functions. While logistic regression is used to develop fragility functions for prevailing different failure modes, that is, floatation and buckling, a Bayesian network methodology has been developed to combine the fragility functions, taking into account common causes and conditional dependencies. The end results have been presented in the form of point estimate total failure probabilities of vessels subject to credible floods. The results of the present study illustrate that although the floatation is the most prominent failure mode in case of floods, the anchorage of target vessels (via bolts), prevent the vessel floatation in almost all cases. In addition, for unanchored vessels, such as atmospheric storage tanks, filling the tanks at least with as much chemicals (hydrocarbone products or chemicals with a density ranging from 650 to 850 Kg/m^3) as equal to the height of flood inundation would significantly reduce the probability of floatation. In case of shell buckling, the height of inundation seems to be a more influential factor than the flow velocity. Besides, it turned out that a small increase in the wall thickness of target vessels would notably decrease the probability of shell buckling.

ECHO/SUB/2015-713844-PREV11 - PEC: Post-Emergency, multi-hazard health risk assessment in Chemical disasters
Project co-funded by ECHO - Humanitarian Aid and Civil Protection

INDEX

INDEX OF FIGURES

INDEX OF TABLES

ECHO/SUB/2015-713844-PREV11 - PEC: Post-Emergency, multi-hazard health risk assessment in Chemical disasters
Project co-funded by ECHO - Humanitarian Aid and Civil Protection

INTRODUCTION

Technological accidents which are triggered by natural events such as earthquakes, hurricanes, floods, and lightings, are known as natech (natural-technological) accidents. The occurrence of natech accidents in chemical and process plants, particularly, can pose disastrous risks to human and the environment due to the release and spread of toxic and flammable chemicals in large quantities. Compared to safety accidents, which are usually a matter of equipment failure or human error, natech accidents can lead to severer consequences owing to the possibility of multiple and simultaneous failures of process vessels, higher likelihood of domino effects, and the damage of infrastructures (e.g., power grids, communication networks, water distribution systems, transportation networks, etc.) required for conducting a timely and effective emergency response (Campedel, 2008; Krausmann and Mushtaq, 2008).

To account for the risk of natech accidents in the quantitative risk assessment of chemical facilities, the correlation between the parameters of a natural event (e.g., the frequency and the peak gravitational acceleration of an earthquake) and the observed damage states of impacted vessels should be identified; the result is usually displayed in form of fragility curves, where the parameter of interest (or a polynomial function of the parameters of interest) and the (cumulative) probability of damage are presented on the abscissa and ordinate axes, respectively (Salzano et al., 2003; Korkmaz et al., 2011; Girgin and Krausmann, 2013).

As opposed to the natech accidents in chemical plants which have been caused by earthquakes or storms (high winds), the ones triggered by floods have received less attention (Campedel, 2008), both in the relevant design standards and regulations (API, 620; API, 650; ASCE-7, 2006; FEMA, 1995) and available literature. This has mainly been due to the rarity of flood-induced natech accidents in general – constituting only 2 to 4% of industrial accidents (Cozzani et al., 2010) – and partly due to the scarcity of historical or experimental data relating the characteristics of floods (frequency of flood, water height, water speed) to the damage states (or failure mode) of impacted equipment.

Figure 1. Flooded railcars and chemical plant in Braithwaite, Louisiana, USA, in the aftermath of Isaac, August 31, 2012 (available at: http://blogs.voanews.com/photos/2012/09/01/september-1-2012).

As pointed out by Campedel (2008), only for a limited number of floods the height of flood inundation have been identified (e.g., see Santella et al., 2010) whereas there are even a lesser number of floods with known water speed. Aside from the lack of detailed data about the floods' characteristics, the available information in the literature about the failure modes and the cause of chemical release is usually qualitative (Godoy, 2007; Campedel, 2008; Krausmann and Mushtaq, 2008; Santella et al., 2010), not determining the severity of damage. Or in most cases, for example, it is not clarified if the chemical release has been due to disconnected pipelines or the structural collapse of the vessel (Cozzani et al., 2010).

Investigating a number of major accident databases throughout Europe and the U.S., Cozzani et al. (2010) identified, based on 272 flood-induced natech accidents from 1960 to 2007, the aboveground storage tanks as the most frequently damaged equipment (74% of cases), including atmospheric storage tanks, floating roof tanks, and pressurized tanks, in a descending order (Figure 2). Besides, the displacement of equipment (due to rigid sliding or floating), shell rupture due to impact with debris, and the collapse of equipment (it has not been defined whether due to overturning or shell buckling) have been identified as the prevailing failure modes (Cozzani et al., 2010).

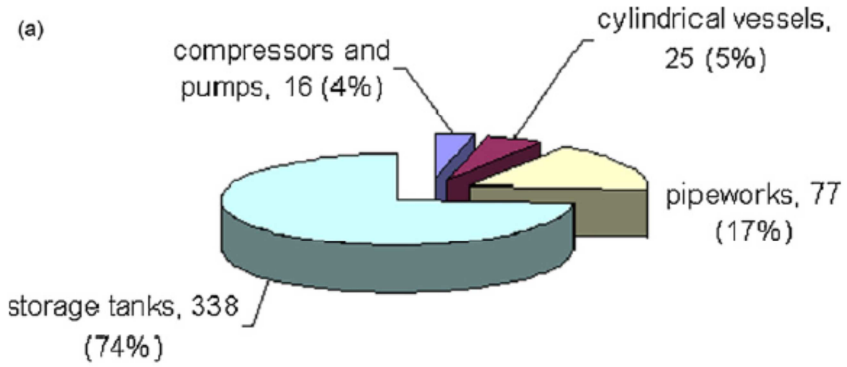

Figure 2. Categories of equipment items involved in flood-induced natechs (Cozzani et al., 2010)

Similar failure modes have been reported in Godoy (2007) based on the site observations of affected process plants in Louisiana and Texas, U.S., following Hurricane Katrina in 2005, where the buckling of tanks' shell was mainly attributed with the strong winds not the ensuing flood (Figures 3 and 4). It is also worth mentioning that the pipeline disconnection as a lateral failure mode resulting from the displacement of equipment has reportedly led to significant chemical releases as well (Godoy, 2007; Campedel, 2008; Cozzani et al., 2010).

Due to the scarcity of historical data with sufficient resolution, the majority of previous quantitative risk assessment studies has relied on analytical or numerical techniques to calculate the probability of failure (modes) based on the failure mechanism (physics of failure) of impacted vessels (Landucci et al., 2012, 2014; Mebarki et al., 2014; Kameshwar and Padgett, 2015).

In almost all previous studies, based on a comparison between the flood-induced forces (loads) exerted on a vessel (e.g., buoyant force of water) and the resistance of the vessel (e.g., weight of the vessel and its contents), limit state equations (LSEs) have been developed for different failure modes of the vessel. Using the LSEs, either the critical values of influential parameters, e.g., the critical height of liquid inside the storage tank to prevent from buckling of the tank shell, have been

determined (Landucci et al., 2012, 2014) or assuming probability distributions for random load-resistance parameters, a number of fragility curves have been developed to correlate the load-resistance parameters to failure probabilities (Mebarki et al., 2014). In a slightly different approach, Kameshwar and Padgett (2015) used LSEs in conjunction with Latin hypercube sampling to generate data required for logistic regression.

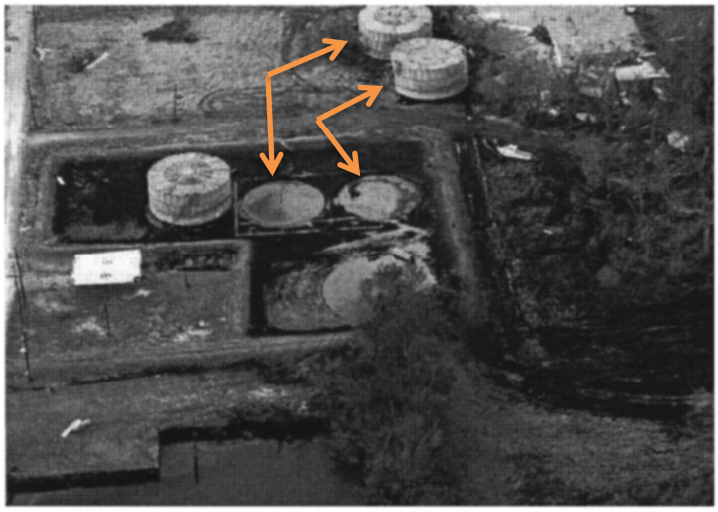

Figure 3. Displacement of storage tanks due to floatation (Godoy, 2007).

Figure 4. Buckling of storage tanks (Godoy, 2007).

In the abovementioned studies, however, the focus has been on a few failure modes and not necessarily the most credible ones (e.g., Landucci et al., 2012). And where more than one failure mode have been investigated (Mebarki et al., 2014; Kameshwar and Padgett, 2015), the resulting fragility functions have been combined deterministically, assuming independent failure modes. This latter oversimplification, however, can significantly compromise the reliability of end results since the same flood-induced loads contribute to all the failure modes of an impacted vessel, making the failure modes and thus the fragility functions heavily correlated.

The present study is aimed at presenting a structured methodology based on previous studies to develop and combine fragility functions for a broader range of flood-induced failure modes. The schematic of the proposed methodology has been illustrated in Figure 5 while the steps taken will be addressed in more detail in the following sections.

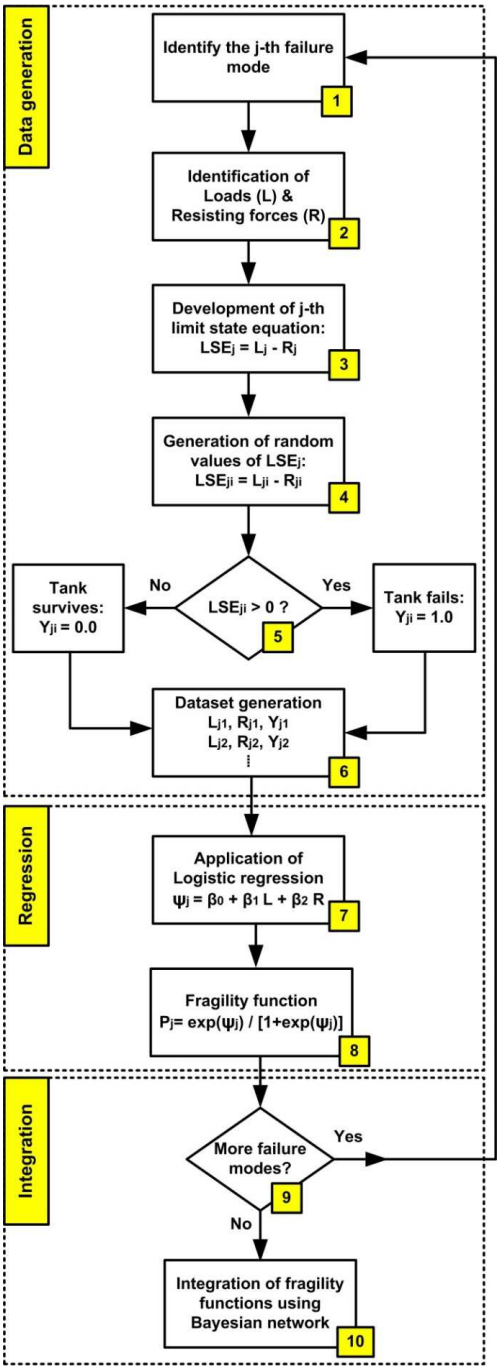

Figure 5. Schematic of the proposed methodology

In Section 2, the failure modes of aboveground atmospheric storage tanks (hereafter, storage tanks) will be modeled using LSEs (Steps 1-3 in Figure 1). These equations will be coupled with Monte Carlo simulation to generate data required to develop fragility functions using logistic regression (Steps 4-6 in Figure 1). In Sections 3 and 4, the basics of logistic regression (used in Steps 7 and 8 in Figure 1) and BN (used in Steps 9 and 10 in Figure 1) will be recapitulated, respectively. The application of the methodology will be demonstrated in Section 5 for aboveground atmospheric storage tanks as a type of equipment having experienced most of failure modes (Godoy, 2007; Krausmann and Mushtaq, 2008; Cozzani et al., 2010). The conclusions are presented in Section 6.

ECHO/SUB/2015-713844-PREV11 - PEC: Post-Emergency, multi-hazard health risk assessment in Chemical disasters
Project co-funded by ECHO - Humanitarian Aid and Civil Protection

2.1. Floatation

Displacement of storage tanks mainly due to floatation has reportedly been the most frequent flood-induced failure mode according to the observations made after the Hurricane Katrina (Godoy, 2007; Santella et al., 2010) and the investigation of major accident databases (Cozzani et al., 2010). As reported by Godoy (2007), displacements of up to 30 m have been recorded due to the flood subsequent to the Hurricane Katrina, causing either pipeline detachment or severe structural damages.

To develop the LSE representing the floatation of a storage tank, the main resisting forces, which are the weight of the tank bulk W_T and the weight of the contained chemical W_L, and the loading force, which is the buoyant force F_B of flood (White, 2003), have been denoted on a typical storage tank in Figure 6, where D, H, and t are the tank's diameter, height, and thickness.

The height of the chemical inside the tank and the water inundation have been denoted, respectively, by h and S. Although the specifications for the anchorage of storage tanks have been given in current standards (e.g., API, 650), the common design practice in many plants is still based on self-anchored storage tanks (Godoy, 2007). Depending on whether the tank is anchored or not, a resisting force F_F provided by the anchorage system (e.g., bolts and the concrete foundation) should also be considered (Kameshwar and Padgett, 2015).

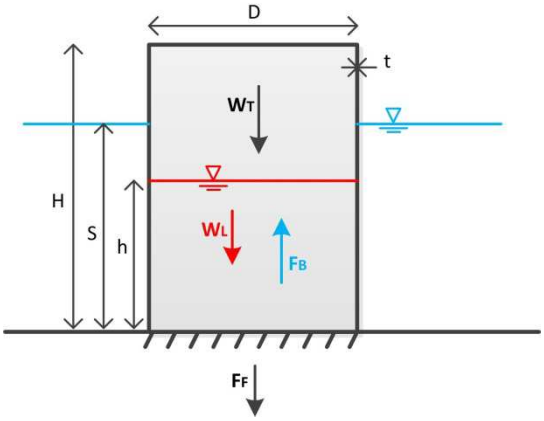

Figure 6. Schematic of the load-resistance forces considered for tank floatation.

Considering the direction of the loading and resisting forces in Figure 6, the floatation limit state equation, $LSE_{Floatation}$, can be developed in Equations (1)-(5):

$$LSE_{Floatation} = F_B - W_T - W_L - F_F \quad (1)$$

$$F_B = \rho_w g \frac{\pi D^2}{4} S \quad (2)$$

$$W_T = \rho_s g \left(\pi DH + 2\frac{\pi D^2}{4}\right) t \quad (3)$$

$$W_L = \rho_l g \frac{\pi D^2}{4} h \quad (4)$$

$$F_F = N_b A_b f_b \quad (5)$$

where ρ_w, ρ_s, and ρ_l are the densities ($\frac{kg}{m^3}$) of the flood water, tank shell (usually steel), and the chemical substance inside the tank, respectively; $g = 9.81 \frac{m}{s^2}$ is gravitational acceleration; N_b is the number of anchorage bolts; A_b is the sectional area (m^2) of each bolt, and f_b is the yield stress of the bolt (Pa).

Equation (5) can further be extended to account for the strength of the concrete foundation holding the bolts as well (Kameshwar and Padgett, 2015). Nevertheless, since the aim of the present study is to develop a methodology rather than rendering case-specific flood-induced fragility functions, the effect of foundation will not be considered for the sake of brevity. As can be seen from Equation (1), the tank will float if $LSE_{Floatation} > 0$. It is also worth noting that the only flood parameter contributing to this failure mode is the height of flood inundation, S.

2.2. Shell buckling

As reported by Godoy (2007), the shell buckling of storage tanks was mainly caused by high winds during the Hurricanes Katrina and Rita rather than by the subsequent flood (in case of Katrina). However, Campedel (2008) and Cozzani et al. (2010) have pointed out the shell buckling as a potential failure mode[1], where an external pressure above the critical pressure P_{cr} leads to the shell collapse.

To develop the LSE of the shell buckling, the main internal (resisting) and external (loading) radial pressures on the shell have been depicted in Figure 7.

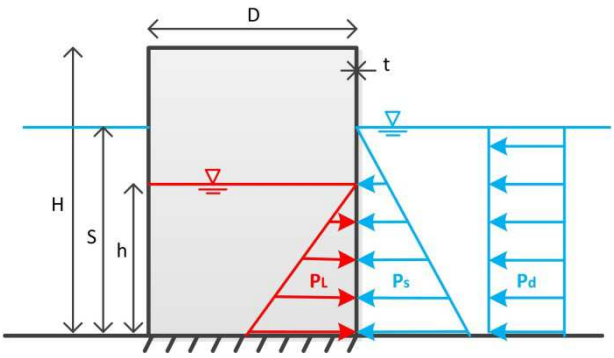

Figure 7. Schematic of the load-resistance forces considered for shell buckling.

These radial pressures include the hydrostatic pressure both from the height of liquid inside the tank P_L and from the height of flood inundation P_s and the hydrodynamic pressure P_d due to the kinetic energy (speed) of the flood flow. Accordingly, the LSE for shell buckling can be developed as Equation (6).

The amounts of hydrostatic pressures P_L and P_s which increase linearly with depth (white, 2003) have been presented in Equations (7) and (8) for the maximum values at the bottom of the tank. To

[1] Actually Cozzani et al. (2010) did not explicitly mention the shell buckling as a failure mode but referred to it via "collapse for instability."

model the hydrodynamic pressure, a uniform distribution can be considered along the water inundation column (ASCE/SEI 7-05, 2006) as presented in Equation (9).

$$LSE_{Buckling} = P_s + P_d - P_L - P_{cr} \quad (6)$$

$$P_L = \rho_l g h \quad (7)$$

$$P_s = \rho_w g S \quad (8)$$

$$P_d = \frac{1}{2} C_d \rho_w V^2 \quad (9)$$

where C_d is the drag coefficient (C_d = 2.0 for square and rectangular piles, and C_d = 1.2 for round piles); V is the average speed of the flow ($\frac{m}{s}$).

For cylindrical shell structures which are subject to radial pressure, the amount of buckling critical pressure P_{cr} (Pa) can be calculated using simplified relationships given in Equation (10) for long cylinders (Iturgaiz Elso, 2012) and in Equation (11) for short cylinders (Landucci et al., 2012), respectively.

$$P_{cr} = \frac{E}{1-v^2}\left(\frac{t}{D}\right)^3 \quad (10)$$

$$P_{cr} = \frac{2Et}{D}\left\{\frac{1}{(n^2-1)\left[1+\left(\frac{2nH}{\pi D}\right)^2\right]^2} + \frac{t^2}{3(1-v^2)D^2}\left[n^2 - 1 + \frac{2n^2-1-v}{\left(\frac{2nH}{\pi D}\right)^2 - 1}\right]\right\} \quad \text{for} \quad n \geq \max\left(\frac{\pi D}{2H}, 2\right) \quad (11)$$

where E is the Young's modulus of the tank material (Pa); v is Poisson ratio; n is the number of waves involved in buckling. As can be seen from Equation (6), the tank shell will buckle if $LSE_{Buckling} > 0$, indicating the net pressure on the shell is beyond the critical threshold. It is also worth noting that the flood parameters S and V both contribute to the buckling failure mode.

2.3. Rigid sliding

As for unanchored storage tanks, the rigid sliding due to the hydrodynamic pressure of the flood surge has been reported as a potential failure mode in Cozzani et al. (2010). Further, as pointed out by Mebarki et al. (2014), both large and small size storage tanks are vulnerable to sliding; for small size storage tanks, sliding is even likelier to cause severer damages than buckling and floatation (perhaps due to the detachment of connected pipelines).

To develop the LSE of sliding, considering the storage tank and its containment as a body of mass, the hydrodynamic force of the flood (load) and the friction force between the tank and the ground (resistance) are taken into account in Equation (12). Accordingly, the hydrodynamic force F_d can be calculated as the product of the hydrodynamic pressure P_d and the vertical wet section area of the storage tank, as shown in Equation (13). The friction force F_{fr} is equal to the product of the friction coefficient C_f and the normal force F_N exerted from the ground to the bottom of the tank, as shown in Equation (14).

For an unanchored storage tank, the normal force is the vector summation of the weight of the tank and its containment and the buoyant force, as shown in Equation (15), yet inasmuch as the tank is

not floated (i.e., $F_N \geq 0$). Having the load, F_d, and the resistance, F_{fr}, the LSE for sliding can be developed as in Equation (12), where $LSE_{Sliding} > 0$ indicates the failure of the tank. As can be noted, both flood parameters S and V contribute to the sliding failure mode.

$$LSE_{Sliding} = F_d - F_{fr} \quad (12)$$

$$F_d = P_d DS \quad (13)$$

$$F_{fr} = C_f F_N \quad (14)$$

$$F_N = W_T + W_L - F_B \quad (15)$$

where C_f is the friction coefficient (0.4 according to API 650).

It should be noted that the existence of the friction force is legitimate as long as the tank stays in touch with the ground; in other words, if the floatation failure mode occurs first, the sliding failure mode will be excluded from the analysis. Such conditional dependency (negative correlation) should be taken into account when integrating these failure modes.

LOGISTIC REGRESSION

Considering a Bernoulli experiment with a binary output variable as Y (0,1), the binomial logistic regression can be used to predict the outcome of the experiment using a probability function $P(x) = P(Y = 1|X = x)$ where X can be a set of parameters (covariates). Having the logistic transformation (or logit) of P(x) as a linear function of x as $ln\frac{P(x)}{1-P(x)} = \beta_0 + \beta_1 x$, the probability function can be presented in Equation (16):

$$P(x) = \frac{e^{\Psi(x)}}{1+e^{\Psi(x)}} \quad (16)$$

where $\Psi(x) = \beta_0 + \beta_1 x$ is the logit function, and β_0 and β_1 are the parameters of the logistic regression, which can be estimated by maximizing the likelihood function of $P(x)$ given an observation of the experiment outcome, as shown by Hosmer et al. (2013) and Van Erp and Van Gelder (2013) using a Bayesian inference scheme. Assuming a Bernoulli experiment (Y=1 if the storage tank fails and Y=0 if the tank does not fail) with a probability distribution of $P(x)$, the likelihood function for n observations can be developed as Equation (17):

$$Likelihood = \prod_{i=1}^{n} P(Y = y_i|X = x_i) = \prod_{i=1}^{n} P(x_i)^{y_i}(1 - P(x_i))^{1-y_i} \quad (17)$$

For the sake of computational simplicity, the natural logarithm of the likelihood function, known as log-likelihood, can be maximized instead of the likelihood function:

$$Log - Likelihood = \sum_{i=1}^{n} y_i P(x_i) + (1 - y_i)(1 - P(x_i)) \quad (18)$$

BAYESIAN NETWORK

Bayesian networks (Pearl, 1988) represent all conditional dependencies (and independencies) among a system's variables by means of joint probability distributions. BNs are acyclic directed graphs in which the systems' random variables (components) are represented by nodes (conventionally, elliptical) while the direct probabilistic dependencies among the nodes are represented by directed arcs. The nodes with arcs directed from them are called parents while the ones with arcs directed into them are called children. The nodes with no parents are also called root nodes, whereas the nodes with no children are known as leaf nodes (Figure 8).

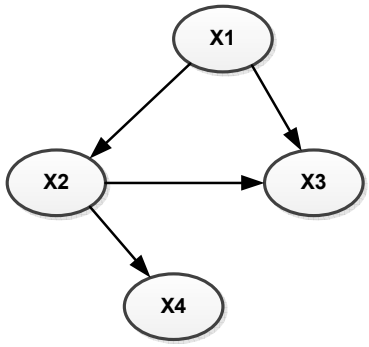

Figure 8.A typical Bayesian network. X_1 (root node) is the parent of X_2 and X_3, and also the ancestor of X_4. X_2 (intermediate node) is the child of X_1 and the parent of X_4. X_3 (leaf node) is the child of X_1 and X_2. X_4 (leaf node) is the child of X_2 and the descendant of X_1.

Satisfying the so-called Markov condition, which states that a node (e.g., X4 in Figure 8) is independent of its non-descendants (e.g., X1 and X3 in Figure 8) given its parents (e.g., X2 in Figure 8, a BN factorizes a joint probability distribution of its random variables (nodes) as a product of the conditional probability distributions of the variables given their parents in the graph:

$$P(X_1, X_2, \dots, X_n) = \prod_{i=1}^{n} P(X_i | Pa(X_i)) \quad (19)$$

where $Pa\ (Xi)$ is the parent set of the variable Xi. For example, considering the BN displayed in Figure 8, $P(X1, X2, X3, X4) = P(X1)\ P(X2|X1)\ P(X3|X1, X2)\ P(X4|X2)$.

The most important type of reasoning in BNs is probability updating given some information, so-called evidence. The evidence is usually in form of observing a random variable(s) be in one of its states. Accordingly, Bayes' Theorem can be employed to propagate the evidence, updating the probabilities of the other nodes conditionally dependent to the observed variable. For example, setting the state of X_4 in Figure 8 to one of its states, $X_4 = x_4^+$, the probability of X_1 being in the state x_1^+ can be calculated using:

$$P(x_1^+ | x_4^+) = \frac{P(x_1^+) P(x_4^+ | x_1^+)}{P(x_4^+)} = \frac{\sum_{X_2, X_3} P(x_1^+, X_2, X_3, x_4^+)}{\sum_{X_1, X_2, X_3} P(X_1, X_2, X_3, x_4^+)} \quad (20)$$

5.1. Vessels specifications

In this study, the fragility of chemical vessels listed in Table 1 is assessed subject to a number of credible floods hitting the plants of interests. For flood-induced fragility assessment of the vessels in Table 1, a comprehensive flood hazard assessment should be performed to identify the frequency of floods along with parameters such as the height of inundation, S, and flow velocity, V. This demands for an exhaustive investigation of mechanisms that can lead to floods, including extreme precipitation, snow melting, and dam breaks, along with the hydrological and topological aspects of floodplains (van Gelder, 2013).

Table 1. Specifications of the process vessels

Unit	H (m)	D (m)	V (m^3)	t (mm)	P_g (KPa)
Storage tanks					
Virgin naphtha storage tank	8	10	500	10	0.0
Cracking Gasoline buffer tank	9	12	1000	10	0.0
Cracking Gasoline storage tank # 1	11	22	5000	10	0.0
Cracking Gasoline storage tank # 2	12	37	15000	10	0.0
Acrylonitrile storage tank	11	15	1500	10	0.0
Latex storage tank	11	15	1500	10	0.0
Vertical vessels					
Primary fractioner	19	8.3	1000	5	190
Heavy gasoline stripper	6.4	1.6	11.8	5	190
Quench column	15	5.7	380	5	190
Debutanizer	16.4	3.2	132	5	190
Horizontal vessels					
Production reactor	3.6	2	20	5	190
Stripping column	4.6	3	50	5	190
Unit buffer vessel	3.1	2	15	5	190

Investigating the historical flood-induced damages in chemical and process facilities, Campedel (2008) determined three types of floods: (i) high water condition, where S > 1m and V= 0.25m/s, (ii) high flow condition, where V > 2 m/s and S= 0.5m, and (iii) high risk condition, where S= 1m and V= 1m/s. In the present study, according to a numerical simulation of the floodplain and the possibility of a dam break, two floods were predicted using two different equations for calculation of released discharged Q resulted from the dam break (please see D.A.2: Flood Hazard Analysis, for more details).

One flood resulted from a Q = 250 m^3/s with a S= 1.44 m and V= 0.4 m/s while the other flood resulted from a Q= 500 m^3/s with a S= 4 m and V= 1.4 m/s. Based on these floods and using a double exponential regression, a number of credible floods were predicted for the floodplain where the chemical plants of interest locate. The predicted floods are reported in Table 2.

Table 2. Predicted flood scenarios.

Flood Scenario	Water Height (m)	Flow Velocity (m/s)	Return period (yr)	Frequency (1/yr)
1	0.5	0.175	5.11	1.96 E -01
2	1.0	0.35	26.1	3.83 E -02
3	1.5	0.525	133.35	7.50 E -03
4	2.0	0.70	681.3	1.47 E -03
5	4.0	1.40	464167	2.15 E -06

5.2. Floatation fragility assessment

To derive the floatation fragility curves of the vessels exposed to the aforementioned floods, Monte Carlo simulation was used to generate random values of $LSE_{Floatation}$ based on Equations (1)-(4). Given a flood, all the parameters were assumed constant (Table 3) except the height of chemicals inside the vessels which was considered to follow a uniform distribution $h \sim Uniform\,(0.0, 0.75H)$. In this regard, the positive values of $LSE_{Floatation}$ was considered as an indication of the vessel floatation, Y= 1.0, whereas negative values were considered as the vessel not being floated, Y= 0.0.

Table 3. Numeric parameters used for the fragility assessment.

Parameter	Symbol	Value	Unit
Tank shell density (steel)	ρ_s	7900	kg/m^3
Flood water density	ρ_w	1024	kg/m^3
Chemical density	ρ_l	720, 810, 876	kg/m^3
Young's modulus	E	2.1 E +11	Pa
Buckling critical pressure	P_{cr}	3.15 E +04	Pa
Yield stress of bolt	f_b	170	MPa
Poisson ratio	v	0.3	
Friction coefficient	C_f	0.4	
Number of buckling waves	n	25	

Corresponding to each random value of h (and thus a random value of $LSE_{Floatation}$), a floatation probability P(h) was predicted using Equation (16) for arbitrarily initial values of β_0 and β_1 (both equal to 0.5 in this study).

Forming a likelihood function for each set of h, Y, and P(h) using Equation (17), the optimal values of β_0 and β_1 were estimated using the maximum likelihood estimation analysis. For illustrative purposes, the floatation fragility curves of the cracking gasoline storage tank # 2 due to the floods of Table 2 are depicted in Figure 9 while the optimal values of regression parameters for all vessels have been listed in Tables 4-7.

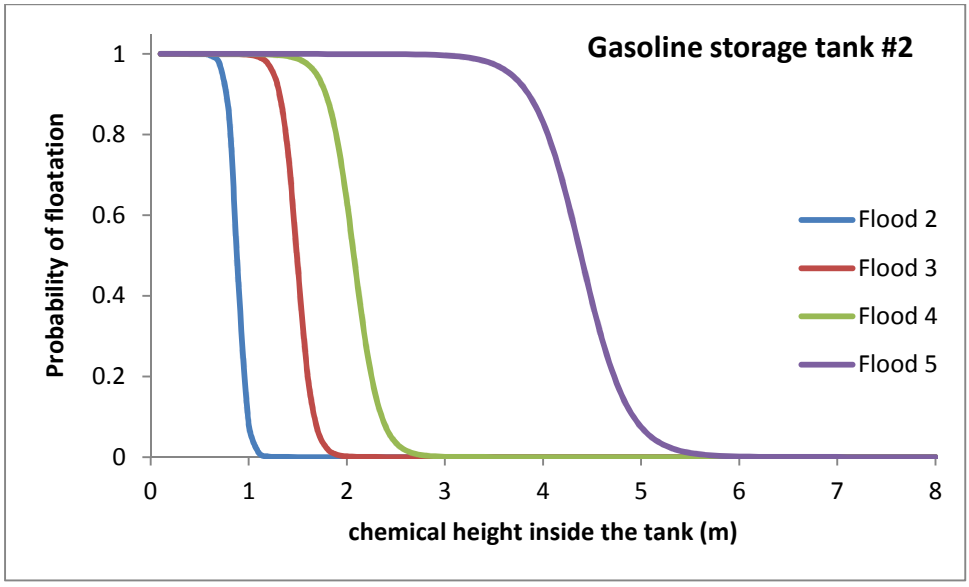

Figure 9. Fragility curves of gasoline storage tank # 2 due to floatation.

5.3. Shell buckling fragility assessment

Following the same procedure, Equations (6)-(9) and (11) can be used to generate random values of $LSE_{Buckling}$ given the flood inundation heights and flow velocities of the floods. For illustrative purposes, the shell buckling fragility curves of the cracking gasoline storage tank # have been depicted in Figure 10.

As can be noted from Figure 10, the flood inundation height seems to play the key role in shell buckling since among the floods the one with a considerable inundation height (Flood 5 with S= 4m) could result in shell buckling even for larger amounts of chemical inside the tank. Such result is in compliance with the observations in Campedel (2008), where high water levels have been attributed to shell instability of atmospheric tanks while high water speeds have been blamed for the failure of the support structures of pressurized tanks.

Moreover, as can be seen in Figure 10, the higher height of chemical content helps significantly reduce the probability of shell buckling, as has been reported in (RRT6, 2016). The optimal values of regression parameters are listed in Tables 4-7.

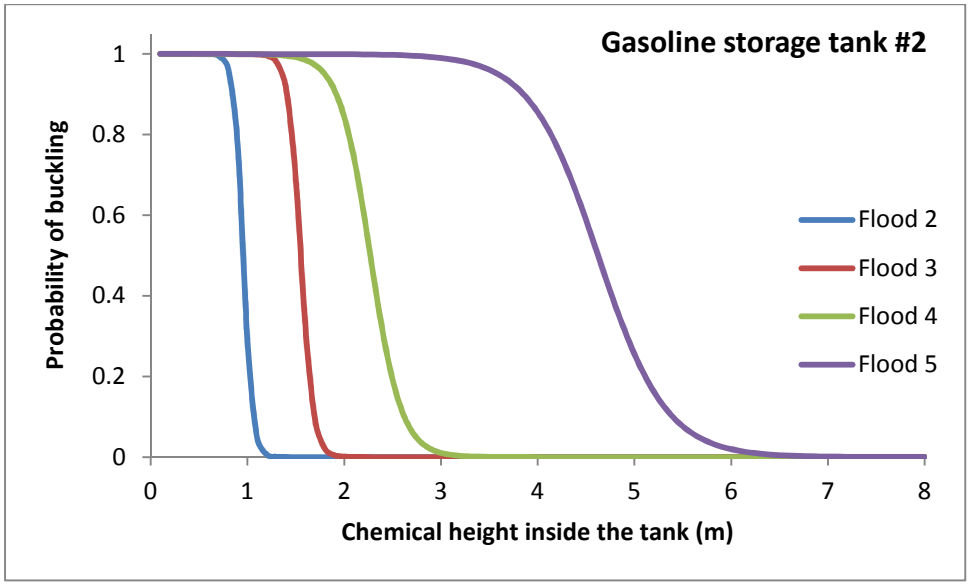

Figure 10. Fragility curves of gasoline storage tank # 2 due to shell buckling.

Table 4. Optimal values of regression parameters β_0 and β_1 used in logit function $\Psi(h)=\beta_0 + \beta_1 h$ for Flood Scenario #2 in Table 2. Na: Not applicable.

Unit	Floatation		Buckling	
	β_0	β_1	β_0	β_1
Virgin naphtha storage tank	20.01	-27.84	Na	Na
Cracking Gasoline buffer tank	20.42	-27.09	Na	Na
Cracking Gasoline storage tank # 1	20.37	-24.29	Na	Na
Cracking Gasoline storage tank # 2	18.21	-20.64	20.18	-21.07
Acrylonitrile storage tank	20.42	-27.09	Na	Na
Primary fractioner	Na	Na	Na	Na
Heavy gasoline stripper	Na	Na	Na	Na
Quench column	Na	Na	Na	Na
Debutanizer	Na	Na	Na	Na
Production reactor	Na	Na	Na	Na
Stripping column	Na	Na	Na	Na
Unit buffer vessel	Na	Na	Na	Na

Table 5. Optimal values of regression parameters β0 and β1 used in logit function $\Psi(h)=\beta 0 + \beta 1 h$ for Flood Scenario #3 in Table 2. Na: Not applicable.

Unit	Floatation		Buckling	
	β_0	β_1	β_0	β_1
Virgin naphtha storage tank	19.57	-14.76	Na	Na
Cracking Gasoline buffer tank	20.26	-14.76	Na	Na

Cracking Gasoline storage tank # 1	20.26	-14.76	14.98	-22.58
Cracking Gasoline storage tank # 2	18.65	-12.51	24.07	-15.51
Acrylonitrile storage tank	20.26	-14.76	Na	Na
Primary fractioner	Na	Na	Na	Na
Heavy gasoline stripper	Na	Na	Na	Na
Quench column	Na	Na	Na	Na
Debutanizer	Na	Na	Na	Na
Production reactor	Na	Na	Na	Na
Stripping column	Na	Na	Na	Na
Unit buffer vessel	Na	Na	Na	Na

Table 6. Optimal values of regression parameters β0 and β1 used in logit function $\Psi(h)=\beta 0 + \beta 1 h$ for Flood Scenario #4 in Table 2. Na: Not applicable.

Unit	Floatation		Buckling	
	β_0	β_1	β_0	β_1
Virgin naphtha storage tank	17.33	-8.89	Na	Na
Cracking Gasoline buffer tank	17.33	-8.89	Na	Na
Cracking Gasoline storage tank # 1	15.99	-7.72	15.07	-11.55
Cracking Gasoline storage tank # 2	15.99	-7.72	14.19	-6.25
Acrylonitrile storage tank	17.33	-8.89	Na	Na
Primary fractioner	Na	Na	Na	Na
Heavy gasoline stripper	Na	Na	Na	Na
Quench column	Na	Na	Na	Na
Debutanizer	Na	Na	Na	Na
Production reactor	Na	Na	Na	Na
Stripping column	Na	Na	Na	Na
Unit buffer vessel	Na	Na	Na	Na

Table 7. Optimal values of regression parameters β0 and β1 used in logit function $\Psi(h)=\beta 0 + \beta 1 h$ for Flood Scenario #5 in Table 2. Na: Not applicable.

Unit	Floatation		Buckling	
	β_0	β_1	β_0	β_1
Virgin naphtha storage tank	18.79	-4.44	Na	Na
Cracking Gasoline buffer tank	18.79	-4.44	Na	Na
Cracking Gasoline storage tank # 1	18.03	-4.11	11.85	-3.16
Cracking Gasoline storage tank # 2	18.03	-4.11	13.18	-2.85
Acrylonitrile storage tank	18.79	-4.44	17.59	-11.34
Primary fractioner	13.71	-11.85	13.77	-5.48
Heavy gasoline stripper	Na	Na	Na	Na
Quench column	Na	Na	Na	Na

Debutanizer	Na	Na	Na	Na
Production reactor	Na	Na	Na	Na
Stripping column*	14.92	-25.24	Na	Na
Unit buffer vessel	Na	Na	Na	Na

* The flotation happens only for a 4-bolt configuration.

5.4. Rigid sliding fragility assessment

As for sliding failure mode, none of the floods could result in the sliding of vessels. This is owing to the fact that for high-water floods (especially Flood 5) a vessel becomes floated before the hydrodynamic force of flood P_d find a chance to cause the vessel to slide whereas for the other floods, not only hydrodynamic force is not notable (due to small flow velocities) but also buoyancy force F_B is not large enough to decrease the normal force F_N and thus the friction force F_{fr} to a sufficiently low amount so as to let P_d slide the tank.

For the sake of clarity, the sliding fragility curve of Virgin Naphtha tank in case of an imaginary extreme flood with S= 1.0m and V= 20m/s has been displayed in Figure 11. As can be seen, even for such an unlikely extreme flood, the probability of sliding is only credible for a limited range of chemical's height inside the tank, $0.84 \leq h \leq 2.84$. As can be noted, for $h < 0.84$ the tank will float (this has been denoted by a vertical dashed line in Figure 11) whereas for $h > 2.84$ the friction force exceeds (due to the increased bulk weight of the tank) the hydrodynamic force and thus no sliding.

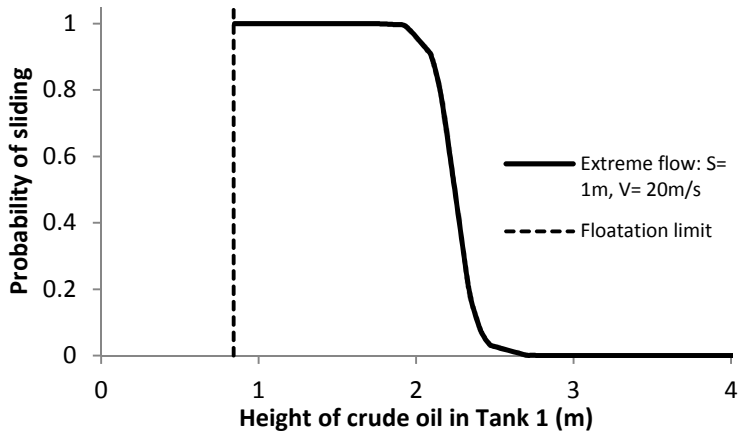

Figure 11. Fragility curve of virgin naphtha storage tank due to sliding in case of an imaginary (very rare) extreme flood.

5.5. Integration of failure modes

Calculating individual fragility functions in the previous sections, a BN (Figure 12) can be employed to combine the failure probabilities, in which the node "Flood" have five states as Flood 1, Flood 2, …, and Flood 5 while the node "h" has discrete states ranging from 0.0 to 0.75h. Having the characteristics of the floods, i.e., S and V, and the states of h, the probabilities of floating and shell buckling can be estimated for the storage tanks and vessels using the regression parameters listed in Tables 4-7.

However, it should be noted that since the failure mode “rigid sliding” would not be caused by any of the floods, it has not been taken into account in the BN.

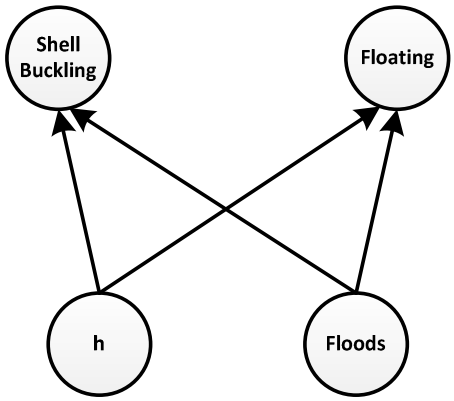

Figure 12. Bayesian network to integrate failure probabilities over possible chemical content and floods.

Using the BN in Figure 12, the total probabilities of floatation and shell buckling of the vessels have been calculated as reported in Table 8.

Table 8. Total probabilities of floatation and shell buckling given the floods in Table 2.

Unit	Floatation	Shell buckling
Virgin naphtha storage tank	4.75E-03	0.00E+00
Cracking Gasoline buffer tank	4.96E-03	0.00E+00
Cracking Gasoline storage tank # 1	5.39E-03	8.07E-04
Cracking Gasoline storage tank # 2	5.71E-03	6.16E-03
Acrylonitrile storage tank	4.96E-03	4.03E-07
Primary fractioner	2.97E-07	6.62E-07
Heavy gasoline stripper	0.00E+00	0.00E+00
Quench column	0.00E+00	0.00E+00
Debutanizer	0.00E+00	0.00E+00
Production reactor	0.00E+00	0.00E+00
Stripping column	1.45E-07	0.00E+00
Unit buffer vessel	0.00E+00	0.00E+00

According to the data analysis carried out by Cozzani et al. (2010), the floatation of a process vessel usually have resulted in a major release and in some cases instantaneous release of chemical contents. On the contrary, the shell buckling has resulted in no release and in cases where the buckling has occurred near a joint connection only minor release of chemicals has been reported. As such, the probabilities listed in Table 8 for the floatation and buckling can be attributed to instantaneous and minor, respectively, release of chemicals.

CONCLUSIONS

In this study we developed a methodology for vulnerability assessment of chemical installations, in subject to floods. The probabilities of individual failure modes such as floatation, buckling, and rigid sliding were estimated in form of fragility curves using logistic regression for which the required data was generated via limit state equations and Monte Carlo simulation.

Considering a number of credible floods for the storage tanks and the vessels of interest, it was illustrated that the floatation is the most prevailing failure mode, especially when the height of chemical inside the vessel is roughly less than the height of flood inundation. It was also demonstrated that the anchorage of vessels with even a minimum number of bolts (4 bolts in this study) can effectively prevent from/reduce the probability of floatation.

For buckling failure mode, however, the height of flood inundation seems to be a more influential parameter than the flow velocity. It was also demonstrated that the probability of buckling can significantly be lowered even with small amounts of containment. It was also demonstrated that atmospheric storage tanks are much more vulnerable to floatation and buckling failure modes compared to pressurized vessels and vertical vessels. As for sliding failure mode, none of regular floods can seem to cause the vessels to slide.

REFERENCES

American Society of Civil Engineers (ASCE). Minimum Design Loads for Buildings and Other Structures. ASCE/SEI 7-05. Reston, Virginia. 2006. ISBN: 0-7844-083 1-9.

API Standard 620. Design and Construction of Large, Welded, Low-pressure Storage Tanks. 12th Edition. American Petroleum Institute Publishing Services, Washington. D.C. 2013.

API Standard 650. Welded Tanks for Oil Storage. 11th Edition. American Petroleum Institute Publishing Services, Washington. D.C. 2007.

Campedel M. Analysis of major industrial accidents triggered by natural events reported in the principal available chemical accident databases. European Commission Joint Research Centre. EUR-Scientific and Technical Research Report: JRC42281. OPOCE. 2008. ISSN: 1018-5593. Available online at http://publications.jrc.ec.europa.eu/repository/handle/JRC42281.

Cozzani V. Campedel M, Renni E, Krausmann E. Industrial accidents triggered by flood events: analysis of past accidents. Journal of Hazardous Materials, 2010; 175: 501-509.

Ebeling C. 2004. An Introduction to Reliability and Maintainability Engineering. Tata McGraw Hill, New Delhi. ISBN-13: 978-0-07-042138-7.

Federal Emergency Management Agency (FEMA). 1995. Engineering principles and practices for retrofitting floodprone residential buildings. FEMA Rep. No. 259, Washington, D.C.

Girgin S, Krausmann E. RAPID_N: Rapid natech risk assessment and mapping framework. Journal of Loss Prevention in the Process Industries, 2013; 26: 949-960.

Godoy LA. Performance of storage tanks in oil facilities damaged by Hurricanes Katrina and Rita. Journal of Performance of Constructed Facilities, 2007; 21(6): 441-449.

Haehnel RB, Daly SF. Maximum impact force of woody debris on floodplain structures. Journal of Hydraulic Engineering, 2004; 130(2): 112-120.

Hosmer D, Lemeshow S, Sturdivant R. 2013. Applied Logistic Regression. 3rd Edition. Wiley & Sons, Hoboken, New Jersey. ISBN: 978-0-470-58247-3.

Iturgaiz Elso M. Finite Element Method studies on the stability behavior of cylindrical shells under axial and radial uniform and non-uniform loads. 2012. Universidad Pública de Navarra, Spain. Available online at http://academica-e.unavarra.es/handle/2454/6186.

Kameshwar S, Padgett JE. Fragility assessment of above ground petroleum storage tanks under storm surge. 12th International Conference on Applications of Statistics and Probability in Civil Engineering, ICASP 12, Vancouver, Canada, July 12-15, 2015.

ECHO/SUB/2015-713844-PREV11 - PEC: Post-Emergency, multi-hazard health risk assessment in Chemical disasters
Project co-funded by ECHO - Humanitarian Aid and Civil Protection

Khakzad N, Khan F, Amyotte P. Safety analysis in process facilities: Comparison of fault tree and Bayesian network approaches. Reliability Engineering and System Safety, 2011; 96: 925–932.

Khakzad N, Khan F, Paltrinieri N. On the application of near accident data to risk analysis of major accidents. Reliability Engineering and System Safety, 2014a; 126: 116–125.

Khakzad N, Khakzad S, Khan F. Probabilistic risk assessment of major accidents: application to offshore blowouts in the Gulf of Mexico. Journal of Natural Hazards, 2014b; 74: 1759–1771.

Khakzad N, Khan F, Amyotte P. Major accidents (Gray Swans) likelihood modeling using accident precursors and approximate reasoning. Risk Analysis, 2015; 35(7): 1336-1347.

Korkmaz K, Sari A, Carhoglu A. Seismic risk assessment of storage tanks in Turkish industrial facilities. Journal of Loss Prevention in the Process Industries, 2011; 24: 314-320.

Krausmann E, Mushtaq F. A qualitative Natech damage scale for the impact of floods on selected industrial facilities. Natural Hazards, 2008; 46: 179–197.

Landucci G, Antonioni G, Tugnoli A, Cozzani V. Release of hazardous substances in flood events: damage model for atmospheric storage tanks. Reliability Engineering and System Safety, 2012; 106: 200-216.

Landucci G, Necci A, Antonioni G, Tugnoli A, Cozzani V. Release of hazardous substances in flood events: damage model for horizontal cylindrical vessels. Reliability Engineering and System Safety, 2014; 132: 125-145.

Mebarki A, Willot A, Jerez S, Reimeringer M, Prod' Homme G. Vulnerability and resilience under effects of tsunamis: case of industrial plants. Procedia Engineering, 2014; 84: 116-121.

Neapolitan R. 2003. Learning Bayesian networks. Upper Saddle River, NJ, USA: Prentice Hall, Inc.

Pearl J. 1988. Probabilistic reasoning in intelligent systems. San Francisco, CA: Morgan Kaufmann.

Region 6 Regional Response Team (RRT6). Flood Preparedness. Recommended Best Practices. FactSheet #103, January 2016. Available online at: http://www.deq.louisiana.gov/portal/portals/0/news/pdf/FloodPrepFactSheetDRAFT.pdf.

Salzano E, Iervolino I, Fabbrocino G. Seismic risk of atmospheric storage tanks in the framework of quantitative risk analysis. Journal of Loss Prevention in the Process Industries, 2003; 16: 403-409.

Santella N, Steinberg LJ, Sengul H. Petroleum and hazardous material releases from industrial facilities associated with Hurricane Katrina. Risk Analysis, 2010; 30(4): 635-649.

Van Erp N, Van Gelder P. Bayesian logistic regression analysis. 32nd International Workshop on Bayesian Inference and Maximum Entropy Methods in Science and Engineering, Garching, Germany, 15-20 July 2012.

Van Gelder P. 2013. Flood Risk Management, Quantitative Methods, in Encyclopedia of Environmetrics, El-Shaarawi and Piegorsch (eds), John Wiley & Sons Ltd: Chichester, UK. DOI: 10.1002/9780470057339.

White F. Fluid Mechanics. 2003. 5th edition. McGraw-Hill, Boston. ISBN-13: 978-0072402179.
Coles DG, Ragaini RC, Ondov JM, et al. 1979. Chemical studies of stack fly ash from a coal-fired power plant. Environ Sci Tech 13(4):455-459.

ECHO/SUB/2015-713844-PREV11 - PEC: Post-Emergency, multi-hazard health risk assessment in Chemical disasters
Project co-funded by ECHO - Humanitarian Aid and Civil Protection